IOP Publishing | International Atomic Energy Agency Nuclear Fusion

Nucl. Fusion **56** (2016) 126010 (8pp) doi:10.1088/0029-5515/56/12/126010

Developing and validating advanced divertor solutions on DIII-D for next-step fusion devices

H.Y. Guo[1], D.N. Hill[1], A.W. Leonard[1], S.L. Allen[2], P.C. Stangeby[3], D. Thomas[1], E.A. Unterberg[4], T. Abrams[1], J. Boedo[5], A.R. Briesemeister[4], D. Buchenauer[6], I. Bykov[5], J.M. Canik[4], C. Chrobak[5], B. Covele[7], R. Ding[1], R. Doerner[5], D. Donovan[8], H. Du[9], D. Elder[3], D. Eldon[10], A. Lasa[4], M. Groth[11], J. Guterl[1], A. Jarvinen[2], E. Hinson[12], E. Kolemen[10], C.J. Lasnier[2], J. Lore[4], M.A. Makowski[2], A. McLean[2], B. Meyer[2], A.L. Moser[1], R. Nygren[6], L. Owen[4], T.W. Petrie[1], G.D. Porter[2], T.D. Rognlien[2], D. Rudakov[5], C.F. Sang[1], C. Samuell[2], H. Si[13], O. Schmitz[12], A. Sontag[4], V. Soukhanovskii[2], W. Wampler[6], H. Wang[1] and J.G. Watkins[6]

[1] General Atomics, San Diego, CA, USA
[2] Lawrence Livermore National Laboratory, Livermore, CA, USA
[3] University of Toronto, Toronto, ON, Canada
[4] Oak Ridge National Laboratory, Oak Ridge, TN, USA
[5] University of California at San Diego, La Jolla, CA, USA
[6] SNL Sandia National Laboratory, Albuquerque, NM, USA
[7] University of Texas at Austin, Austin, TX, USA
[8] University of Tennessee, Knoxville, TN, USA
[9] Dalian University of Technology, Dalian, Liaoning, People's Republic of China
[10] Princeton University, Princeton, NJ, USA
[11] Aalto University, 02015 Espoo, Finland
[12] University of Wisconsin, Madison, WI, USA
[13] Institute of Plasma Physics, Hefei, Anhui, People's Republic of China

E-mail: guohy@fusion.gat.com

Received 29 April 2016, revised 15 June 2016
Accepted for publication 5 July 2016
Published 14 September 2016

Abstract

A major challenge facing the design and operation of next-step high-power steady-state fusion devices is to develop a viable divertor solution with order-of-magnitude increases in power handling capability relative to present experience, while having acceptable divertor target plate erosion and being compatible with maintaining good core plasma confinement. A new initiative has been launched on DIII-D to develop the scientific basis for design, installation, and operation of an advanced divertor to evaluate boundary plasma solutions applicable to next step fusion experiments beyond ITER. Developing the scientific basis for fusion reactor divertor solutions must necessarily follow three lines of research, which we plan to pursue in DIII-D: (1) Advance scientific understanding and predictive capability through development and comparison between state-of-the art computational models and enhanced measurements using targeted parametric scans; (2) Develop and validate key divertor design concepts and codes through innovative variations in physical structure and magnetic geometry; (3) Assess candidate materials, determining the implications for core plasma operation and control, and develop mitigation techniques for any deleterious effects, incorporating development of plasma-material interaction models. These efforts will lead to design, installation, and evaluation of an advanced divertor for DIII-D to enable highly dissipative divertor operation at core density (n_e/n_{GW}), neutral fueling and impurity influx most compatible with high

performance plasma scenarios and reactor relevant plasma facing components (PFCs). This paper highlights the current progress and near-term strategies of boundary/PMI research on DIII-D.

Keywords: divertor concept, plasma-material interactions, DIII-D, advanced tokamak, fusion reactor

(Some figures may appear in colour only in the online journal)

1. Introduction

The path towards next-step fusion development requires increased emphasis on the plasma-material interface, or plasma-material interactions, also known as PMI. One of the major issues facing the design and operation of next-step high-power steady-state fusion devices is the control of the heat flux and erosion of the plasma-facing components (PFCs). Advanced divertor solutions to efficiently dissipate heat from fusion reactors are critical, because the maximum steady-state power load is limited to $q_t \leqslant 5$–10 MW m^{-2} to any PFCs, whether solid or liquid. Adequate reactor lifetime dictates near zero-erosion at solid PFCs, hence the divertor plasma temperature at the plasma materials interface, especially at the divertor target plates, must be maintained at a low temperature with $T_e \leqslant 5$ eV to suppress erosion. In addition, these boundary plasma conditions must be maintained at a core plasma density and neutral and impurity influx consistent with robust H-mode operation, efficient current drive, density control and He ash removal. This poses a great challenge for the next-step fusion devices, such as a fusion nuclear science facility (FNSF) [1] or a China fusion engineering test reactor (CFETR) [2], which target relatively lower plasma density than projected from present tokamaks, i.e. a Greenwald density fraction, $n_e/n_{GW} \sim 0.5$, in contrast to $n_e/n_{GW} = 1$ for ITER.

In response to this challenge, the DIII-D National Fusion Program has recently launched an new initiative to develop the physics basis for defining a validated divertor solution to provide power and particle control for steady-state high performance tokamak operation in next-step fusion devices. Such a divertor concept ultimately requires:

- Highly dissipative operation, limiting surface heat and erosion to a tolerable level;
- controlled density, neutral fueling, and impurity influx compatible with high performance core plasma operation;
- use of materials appropriate for a fusion reactor environment of high neutron fluence and temperature.

Achieving this goal requires coordinated effort between experiment and theory to develop and validate predictive physics models and design codes, since the complexity and reach of integrating design choices into a capable divertor for fusion lies well beyond the capability of simplified models or empirical scaling relationships. Progress here requires efficient platforms for conducting simulation, and state-of-the-art tools for comparing data and simulation in a useful way. DIII-D provides a capable platform for conducting such research, having a comprehensive diagnostic set, flexible divertor geometry and wide range of boundary plasma parameter space [3].

Advancing scientific understanding and validating complex simulation codes for use in divertor and PFC design activities requires a systematic approach encompassing both targeted diagnostic development and plasma parameter scans, as well as systematic tokamak modifications. The latter is essential in the design of clean experiments to calibrate simulations and quantify the key physical processes governing radiative dissipation and plasma detachment (e.g. differentiate the effect of neutral reflection/trapping from magnetic flux expansion). Such modifications include not only varying the shape and extent of surrounding structures (i.e. baffles for neutrals), but the target plate inclination relative to magnetic flux surfaces, and the expansion and flaring of the flux surfaces themselves, as well as the magnetic topology near the X-points. Experiments in DIII-D utilize two divertors and a flexible control system allowing independent operation of each, consistent with different divertor configurations. This provides direct divertor comparisons in a single device, in a configuration compatible with advanced tokamak (AT) operation.

Ultimately, successful divertor and PFC design choices should facilitate achieving conditions needed for producing high fusion gain, most notably by providing reliable density and impurity control. PFC material choices for fusion are presently highly uncertain, and materials research is a high priority for next-step fusion development, following two broad lines of research. With tungsten (W) as a leading candidate, experiments in linear simulation facilities characterizing the impact of plasma bombardment on W must be coupled with material exposure in tokamaks to validate the results and to explore additional effects, e.g. transients due to ELMs and disruptions. Complementary experiments examining the effect of PFCs on plasma performance due to material sputtering, erosion, and migration can only be carried in high performance tokamaks. DIII-D, with all-carbon walls and a broad suite of edge/divertor diagnostics, can conduct both types of experiments because effects can be localized and materials can be easily inserted and removed using sample stations, while operating high performance AT discharges.

The goal of this research is to demonstrate highly dissipative divertor operation with reactor relevant PFCs while simultaneously maintaining high performance AT core plasma scenarios. In the remainder of this paper, we highlight the current progress and near-term plan on boundary/PMI research in DIII-D.

2. Advance physics understanding and predictive capability

Advancing physics understanding and developing validated predictive capability is not only necessary for providing the quickest and most economic route to optimization of fusion energy production, but is also essential because it is not possible to match all reactor-level parameters in the divertor, pedestal and core plasmas in present experimental devices and ITER. Existing models require further development to achieve this goal due to the tightly coupled physics processes that must be modeled over a range of spatial and temporal scales. These physical processes include:

- Dissipation of energy and momentum through atomic, molecular and neutral-ion physics;
- Perpendicular and parallel plasma transport, due to turbulence, drifts, and kinetic effects;
- Plasma-material interactions setting boundary conditions for the SOL and divertor plasma.

DIII-D already provides key data for boundary plasma model validation. The facility features a comprehensive set of divertor diagnostics, as shown in figure 1, including the divertor Thomson scattering (DTS) capable of measuring electron density and temperature, n_e and T_e from the target to the X-point and 2D divertor coherence imaging system to measure plasma flow, V_i, and ion temperature, T_i. Fully 2D measurements of density and temperature throughout the inner and outer divertors by DTS have been accomplished in DIII-D, for the first time, in H-mode plasmas, showing directly the impact of plasma drifts on the in–out divertor plasma asymmetry and onset of detachment [4]. Figure 2 shows the 2D maps of divertor n_e and T_e for both forward (normal) and reverse $\mathbf{B}_T$ directions, respectively. The divertor plasma exhibits a higher n_e and lower T_e in the inner divertor than outer for the normal $\mathbf{B}_T$ direction (ion $\mathbf{B} \times \nabla B$ drift toward the bottom divertor). Reversing $\mathbf{B}_T$ mitigates and even reverses the in–out divertor asymmetry. For the particular case shown in figure 2, the detachment occurs in the inner divertor where T_e drops below 1 eV at the inner target for the normal $\mathbf{B}_T$ direction, but becomes reattached in reverse $\mathbf{B}_T$. UEDGE modeling with a full physics drift model has qualitatively reproduced the in–out divertor asymmetry, figure 3, showing important role of $\mathbf{E} \times \mathbf{B}$ drifts on the target asymmetries [5]. The change in the in–out asymmetry is traced to the $\mathbf{E}_r \times \mathbf{B}$ poloidal particle flow under the X-point coupled with the $\mathbf{E}_p \times \mathbf{B}$ radial flow in the divertor legs, where $\mathbf{E}_r$ and $\mathbf{E}_p$ are the radial and poloidal electric fields. $\mathbf{E}_r \times \mathbf{B}$ poloidal drift feeds the inner divertor, while $\mathbf{E}_p \times \mathbf{B}$ radial drift shifts profiles to smaller major radius, for forward $\mathbf{B}_T$, with opposite trends for reverse $\mathbf{B}_T$, in agreement with the experimental observations.

Further investigation has been carried out on DIII-D to examine the impact of non-axisymmetric magnetic field perturbations, in particular, the applied resonant magnetic perturbation (RMP) fields for the control of ELMs, on the heat deposition on the divertor target plates [6], which is presently a serious concern for ITER divertor operation. Previous

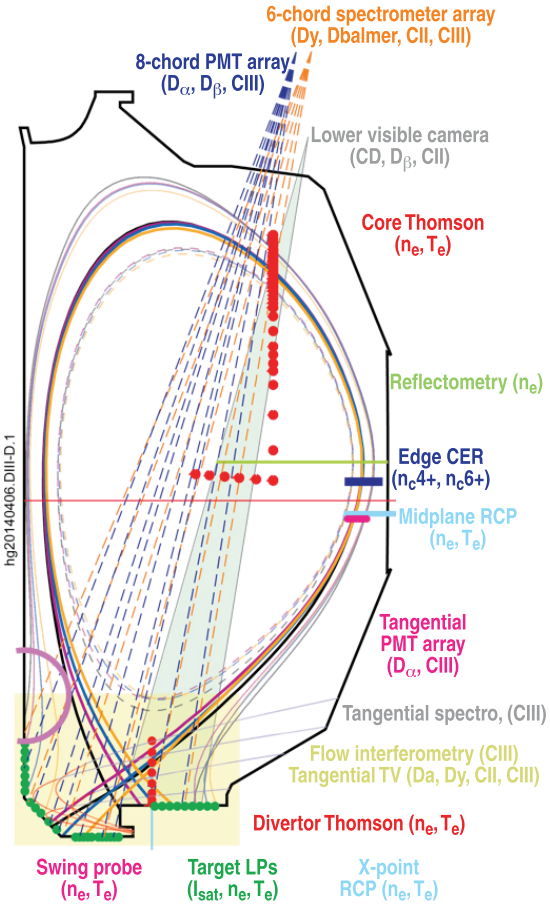

Figure 1. Sketch of boundary/PMI diagnostics on DIII-D.

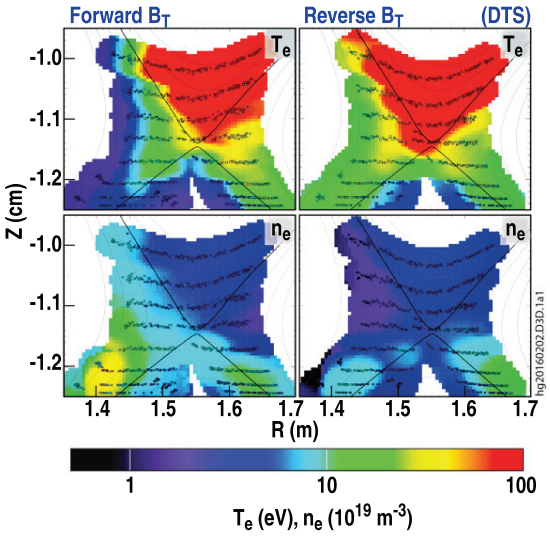

Figure 2. T_e and n_e measured by DTS for two matched H-mode discharges in forward and reverse $\mathbf{B}_T$ with n_e/n_{GW} ~ 0.67 and 0.61, respectively.

results from DIII-D showed that the amplitude of the 3D heat flux striations between ELMs induced by RMP fields increased with the upstream density [7]. New measurements show that at sufficiently high densities, above the onset of divertor detachment, the 3D heat flux striations induced by RMP fields between ELMs can be eliminated and the target

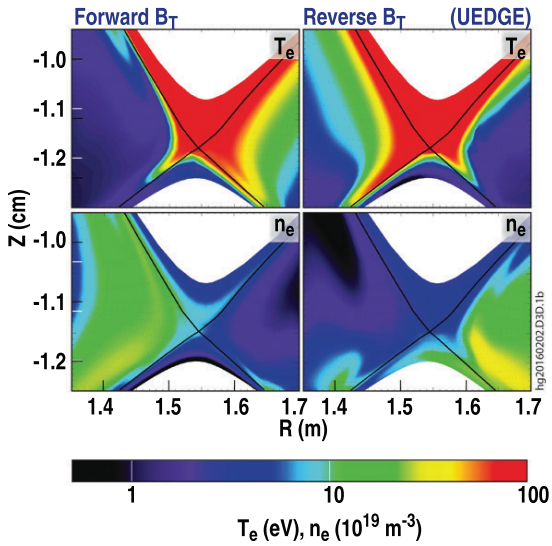

Figure 3. T_e and n_e predicted by the UEDGE code for the H-mode discharges shown in figure 2 with full drifts.

heat flux profile is nearly identical to that measured without RMPs, as shown in figure 4.

Developing power handling solutions requires comprehensive understanding of detachment physics under conditions and geometries relevant to next-step tokamaks. While existing simulation codes can reproduce some salient features of divertor detachment, predictive quantitative agreement with experimental measurements remains a challenge. In particular, 2D or 3D simulation efforts must incorporate nonlinear atomic and molecular physics, proper transport and plasma-wall interactions into computational packages. To illustrate this, figure 5 compares the electron temperature measured by DTS as a function of the poloidal distance along the field lines from the outer strike point. The code reproduced the measurements away from the target, but did not accurately capture the detailed detachment dynamics in the proximity of the divertor target, i.e. as the plasma approaches detachment with $T_e \leqslant 1$ eV at the target. In order to reproduce the measured temperature profile, the total radiation has to be increased by ~2 times in the code [8, 9]. The origin of this discrepancy is not yet understood, and is subject to further investigation.

Further enhancements to diagnostic capabilities are proposed to isolate and quantify the physical processes that a predictive model must describe, including improved spatial and temporal measurements of 2D profiles of n_e, T_e and radiation in order to constrain the modeling of atomic physics and plasma transport processes; ion temperature measurements to determine the power and momentum carried by ions (the dominant loss channels in detached plasma), and enhanced neutral density and impurity measurements in order to quantify the role of neutral particles and impurities in divertor dissipation, as well as improved diagnostics and new tools to monitor PMI effects. These increased capabilities can support and should benefit from an expanded effort in 2D boundary model development and validation in the U.S. and abroad.

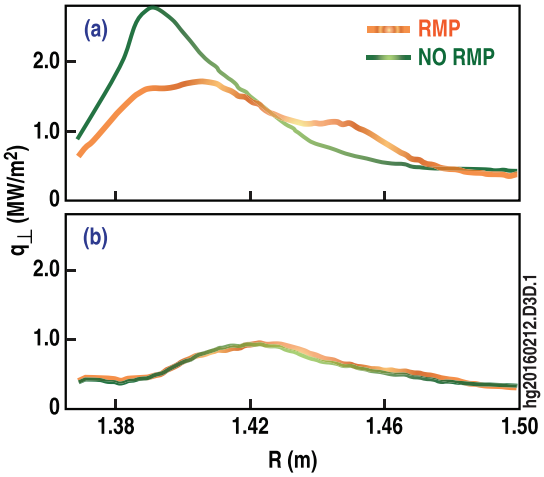

Figure 4. Inter-ELM heat flux profiles at the DIII-D outer divertor target with and without the application of RMP for (*a*) $n/n_{GW} = 0.6$, prior to detachment, and (*b*) $n/n_{GW} = 0.9$, during detachment.

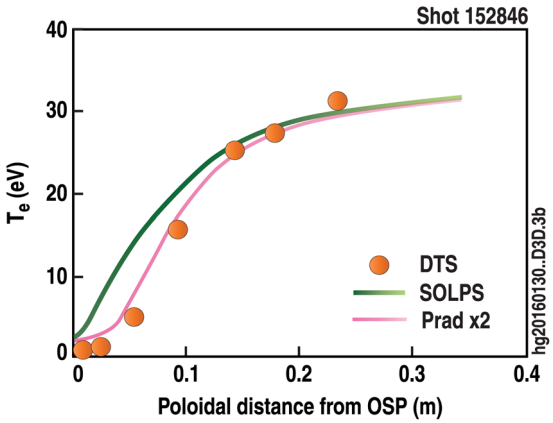

Figure 5. Comparison between DTS measurements and SOLPS modeling: T_e versus the poloidal distance along field lines from the outer strike point.

3. Develop and validate innovative divertor design concepts

The goal of advanced divertor development is to achieve stable, highly dissipative/detached divertor operation across the divertor target at the low upstream density, neutral fueling and impurity influx required for high performance reactor plasmas. The desired normalized core density, n_e/n_{GW}, and/or impurity density, is lower for high performance steady-state reactor plasmas compared to existing tokamaks, primarily due to current drive requirements. Advanced divertor configurations include, (i) a slot divertor [10] with increased divertor volume through divertor leg length, (ii) a snowflake divertor (SFD) [11] to enable heat flux spreading over multi-strike points with a larger X-point region of low poloidal field, which may promote radial transport, i.e. via the 'churning' instability [12], (iii) an X-divertor (XD) [13] with poloidal field flaring near the target to induce stable divertor detachment, (iv) a super-X divertor (SXD) [14] with the divertor target at a larger major radius, and (v) an X-point target divertor (XTD), which is most related to SXD but with an X-point in the divertor leg to create a 'virtual target' [15].

Divertor design choices include divertor target and baffle geometry to direct and confine recycled neutral particles for enhanced dissipation, and magnetic configurations to promote divertor detachment and stable operation. The goal is to reduce the divertor target heat flux, expressed as $q_{\text{target}} = \frac{(1-f_{\text{rad}})P_{\text{SOL}}\sin(\theta_{\text{div}})}{4\pi R_{\text{target}}\lambda_q f_{\text{exp}}}$, where f_{rad} is the radiative power fraction in the SOL and divertor; P_{SOL} is the power flow into the SOL, allowing for radiative loss from the confined plasma; θ_{div} is the angle between the poloidal flux surface and target plate; λ_q is the radial decay length of the SOL heat flux at the outer midplane; and f_{exp} is the poloidal flux expansion factor. Specifically, divertor optimization requires:

(1) Optimizing divertor geometry, i.e. through target plate orientation (θ_{div}) and baffle shaping to improve heat exhaust and enhance the divertor retention for neutrals and impurities to improve particle exhaust and reduce impurity contamination;
(2) Optimizing magnetic configuration to maximize the divertor volume by increasing the wetted area $2\pi R_{\text{target}}\lambda_q f_{\text{exp}}$, through poloidal flux expansion, and the field-line length;
(3) Active radiation and particle control by injecting highly radiative impurities to enhance divertor radiation (f_{rad}), and to reduce the power flow into the divertor (P_{SOL}), i.e. via increasing core/edge radiation.

The configuration flexibility of the DIII-D tokamak will be used to explore and quantify key divertor design parameters controlling divertor detachment and energy dissipation. DIII-D features two divertors with different structures: an open divertor at the bottom and a relatively-closed divertor at the top. Experiments will examine the effect of divertor closure using the upper divertor to maximize neutral entrapping and minimize core performance degradation, while exploring advanced magnetic configurations with the lower divertor, including the SFD and XD configurations (figure 6), leveraging DIII-D's flexible poloidal field coils and robust control system, to provide insight and guidance for the development of a fully optimized divertor concept in DIII-D.

Promising progress has been made on DIII-D in developing the SFD divertor configuration, demonstrating that SFD significantly reduces peak heat fluxes in both attached and radiative divertor regimes, between and during edge localized modes (ELMs), while maintaining good H-mode confinement [16]. The real-time SFD detection and control system has also been developed on DIII-D to stabilize and manipulate this configuration [17]. In addition, we have recently started to explore the XD configuration [13], taking advantage of the open structure of the bottom divertor and the flexible plasma control system. Initial XD experiments on DIII-D exhibit considerable benefits over standard divertor (SD) geometries, both for target heat flux reduction and detachment facilitation [18].

One of the routes identified for advanced divertor operation involves the optimization of baffle shaping [19, 20]. To examine the effect of divertor closure on the onset of divertor detachment in DIII-D, a comparison has recently been made with the lower open divertor to that with the closed upper divertor [21]. The two

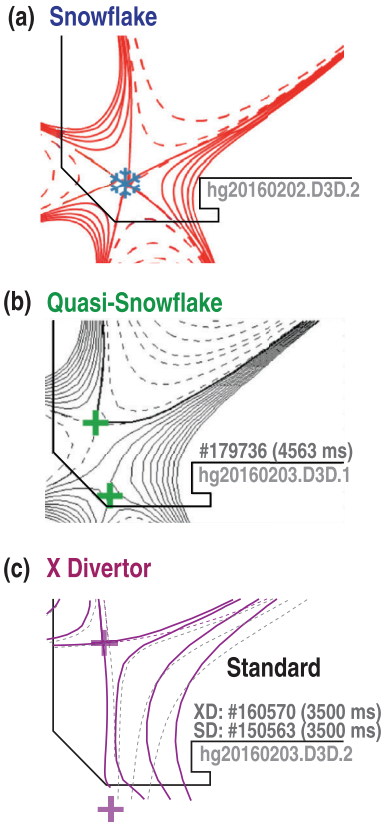

Figure 6. Advanced divertor configurations: (a) ideal snowflake with a large X-point region of low poloidal field; (b) quasi-snowflake (or snowflake minus) with an additional X-point near in the SOL; (c) X-divertor with poloidal flaring near the target.

divertor configurations were run with the same plasma shape, relative $\mathbf{B}\times\nabla B$ drift direction and other operational parameters. As expected, increasing divertor closure with the upper divertor appears to facilitate the onset of detachment, as indicated by the ion saturation current measured by the Langmuir probes at the outer divertor targets, $j_{\text{s,OSP}}$, see figure 7. The rollover of $j_{\text{s,OSP}}$, consistent with momentum loss [22], is indicative of detachment onset. Clearly, the rollover of $j_{\text{s,OSP}}$ occurs at a significant lower plasma density at the pedestal, $n_{\text{e,ped}}$, for the closed upper divertor. Increased closure with the upper divertor improves the confinement of neutrals in the divertor. As a result, the pedestal density profile obtained with the closed upper divertor is significantly lower with a shallower gradient compared to the open lower divertor, as shown in figure 8. This allows the temperature pedestal to grow wider and reach a higher value.

A number of experimental and code studies have shown that modest changes near the target can improve divertor performance significantly, for example [19, 23, 24]. Figure 9 shows two of the slot divertor configurations modeled by SOLPS for test at the upper divertor in DIII-D [25]. The code predicts that in moving from the standard 'flat' to the 'slanted' target configuration, both electron temperature and heat flux at the target, T_{et} and $q_{\perp}$, are dramatically reduced by effectively redirecting and confining recycling neutrals and impurities near the corner, thus enabling the divertor plasma to initiate detachment at a significant lower upstream plasma density, n_{es}, as shown in figure 10.

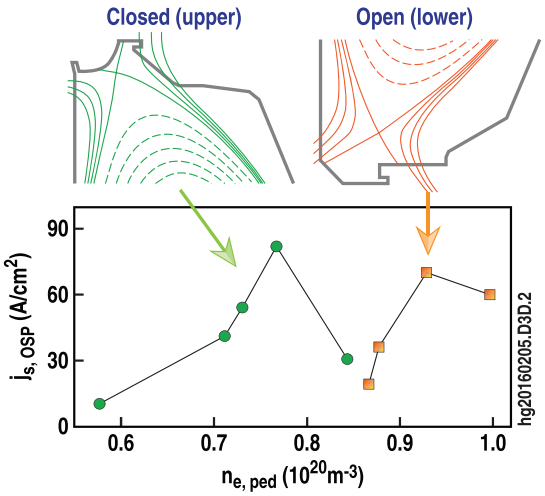

Figure 7. Ion saturation current measured by the Langmuir probes at OSP, $j_{s,OSP}$, as a function of pedestal electron density, $n_{e,ped}$, for the open lower divertor and the closed upper divertor in DIII-D.

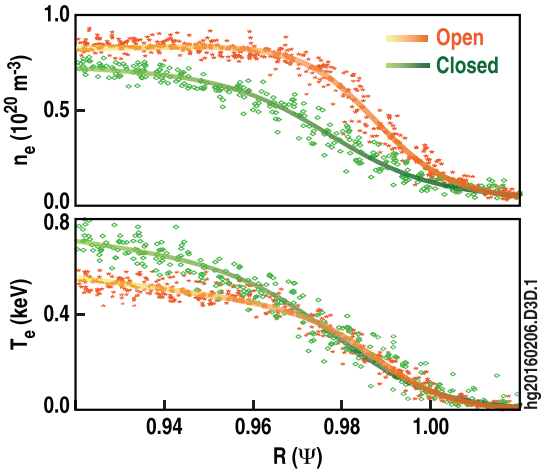

Figure 8. Effect of divertor closure on pedestal profiles of n_e and T_e for the open lower divertor and the closed upper divertor.

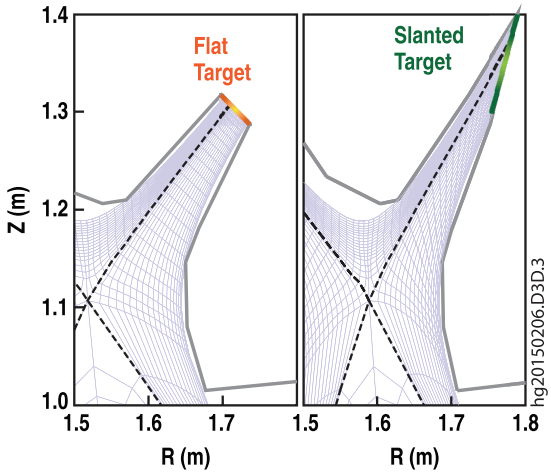

Figure 9. Potential narrow slot divertor options for test on DIII-D.

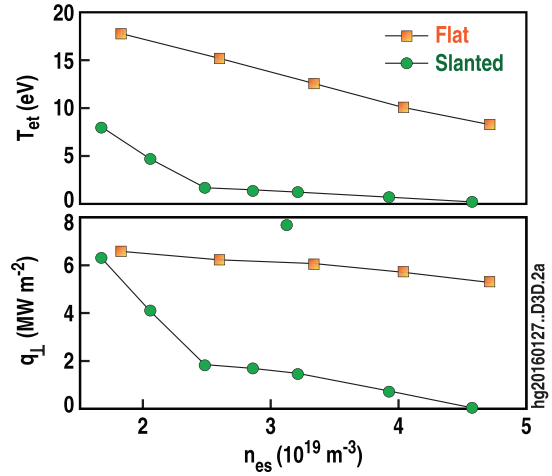

Figure 10. T_e and $q_\perp$ at OSP as a function of the upstream separatrix density, n_{es}, predicted by SOLPS for the flat target and 'slanted' target, respectively, assuming a power flow across the separatrix, $P_{SOL} = 3$ MW.

We are planning to systematically explore and quantify the capability of these divertor configuration options to achieve high divertor dissipation at lower core plasma and impurity density. We will stage divertor structure modifications and magnetic shaping capabilities, guided by the improved models described above, to arrive at an optimized configuration. We will first improve the degree of divertor closure of the upper divertor in the near future by simply reshaping the upper divertor tiles to better confine neutral particles, then iterate/optimize the upper divertor configuration based on further predictive modeling to obtain robust detachment at lower core plasma density, considering (i) target plate tilt and SOL baffling, (ii) private flux baffling, (iii) inner divertor optimization, (iv) additional divertor gas puffing locations, and (v) divertor pumping configuration. As an added benefit the geometry variations will provide clear parameter scans essential for model development and validation. In addition, we will further explore advanced magnetic configurations, including SFD, XD, XTD and SXD, in the lower divertor with enhanced capability to independently control two X-points in the divertor region. These variations are necessarily coupled to some degree, but the proposed staged approach and use of two separate divertors in a single tokamak will provide a clean and well-diagnosed comparison with simulation unobtainable by other means.

4. Evaluation of reactor-relevant PMI solutions

PMI remains a major challenge for successful operation of fusion reactors. Reliable, long-lived PFCs must be developed for next step devices and are a universal challenge to fusion energy, regardless of confinement concept. DIII-D plans to study the impact of the tokamak boundary plasma on advanced materials and to evaluate the impact of materials on the confined plasma. Close collaboration with linear materials testing facilities provides integrated systems testing of candidate materials and components from inception to utilization, including exposure to off-normal plasma events and a broad spectrum of plasma energy and particle-fluxes. Toroidal devices like DIII-D, with pulse lengths ~10 s, provide a very

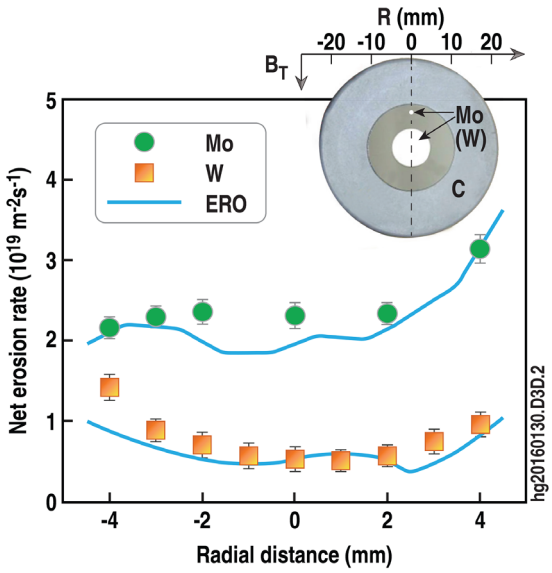

Figure 11. Profiles of net erosion rates for Mo and W between experiments and ERO modelling. Also shown is the photograph of the samples in a graphite DiMES holder.

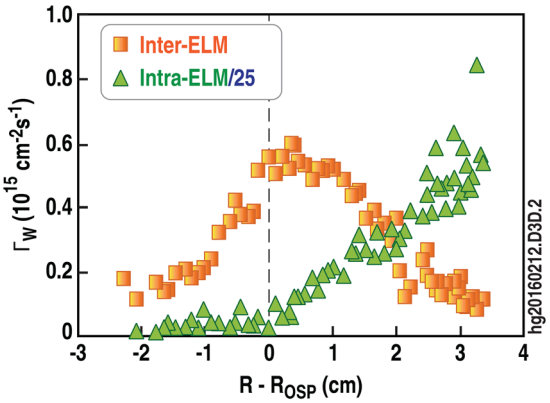

Figure 12. Profiles of W erosion rates at the divertor target during the intra-ELM and inter-ELM phases of H-mode plasmas with the ELM frequency of ~30 Hz in DIII-D.

efficient and cost effective near-term testing platform for plasma exposure, offering relatively easy access, a controlled and realistic environment, and comprehensive diagnosis.

DIII-D is preparing to address the PMI challenge as part of a national research initiative by providing a flexible, well-diagnosed environment for materials evaluation and integrated testing. PMI physics can be appropriately divided into two types: (1) local PMI effects, including surface morphology, erosion, redeposition, hydrogenic retention and recycling from the wall surface; and (2) global plasma effects, including impurity transport, migration and core accumulation. Within this context, DIII-D is proposing increased emphasis on three research thrusts:

- Validation of PMI models for material erosion, redeposition and migration, surface morphology evolution, and hydrogenic recycling in a realistic fusion environment;
- evaluation of the impact of candidate PFC materials on high performance tokamak operation and development of mitigation strategies for deleterious effects;
- assessing the impact of high temperature operation ($T_{surface} \geqslant 500$ °C) on plasma surface interactions and core plasma performance.

The near-term research focus will be the quantitative study of erosion, redeposition and migration of high-Z materials. Addressing the basic physics issues of high-Z material erosion and migration is facilitated by DIII-D's carbon PFCs since high-Z materials are truly trace elements. We have so far been concentrating on the study of local PMI effects, and have recently made significant progress in understanding high-Z material surface erosion and redeposition. Dedicated DIII-D experiments coupled with modeling highlight the roles of the sheath potential, $\mathbf{E} \times \mathbf{B}$ drift and background impurities in determining net erosion of high-Z materials [26]. Figure 11 shows the net erosion profiles of Mo and W samples exposed to the divertor plasmas using the divertor materials evaluation system (DiMES), measured post-mortem by ion beam analysis, along with the calculations by the 3D Monte Carlo code ERO. The modeling has revealed that the net erosion rate is significantly reduced due to the high local re-deposition ratio of eroded materials, which is mainly controlled by the electric field and plasma density within the magnetic presheath. For typical L mode conditions in DIII-D, the net erosion rate of Mo is about 61% of the gross erosion rate, while the net erosion rate of W is only about 33% of the gross erosion rate. Influx spectroscopy can provide important information on source mechanisms [27, 28]. We have recently quantified the impact of ELMs on the tungsten source distribution near OSP with exposures of graphite DiMES probes coated with thin tungsten layers in H-mode discharges. An interesting finding is that the peak W erosion during ELMs is shifted away from the strike point, dramatically broadening the erosion profile at the divertor target due to an underlying shift/broadening of the ion flux during ELMs [29]. As shown in figure 12, the inter-ELM W influx, Γ_w, predominantly arises from the proximity of the OSP ($0 < R - R_{OSP} < 2$ cm), steadily decreasing farther outboard, while the intra-ELM Γ_w peaks in the far SOL.

We will further extend our efforts to evaluate and control the impact of large-scale candidate material PFCs on the plasma performance. We will install toroidal rings of tiles, first with natural W and its isotope (W^{182}) at the divertor entrance and the outer strike zone in June 2016, followed with tests at other strategical locations; this will provide critical data on sputtering sources and erosion due to steady-state and transient loads and their effect on high performance plasmas. In the longer term, materials and component solutions developed by the fusion community will be implemented and evaluated in DIII-D, leveraging its unique capability not only to test the proposed PFC solutions for relevant tokamak conditions, but also to evaluate their compatibility with high performance AT operational regimes.

In addition, we are planning to take a staged approach to assess the impact of high temperature operation on material surface, starting with heated DiMES samples, followed with heated tile-sized samples to evaluate PMI temperature dependence on the size scale of the divertor radial footprint and prototype larger scale heated components.

5. Design of an optimized, integrated divertor solution on DIII-D

Progress on the initiatives described here will inform the design of future divertors on DIII-D to enable highly dissipative divertor operation at core density (n_e/n_{GW}), neutral fueling and impurity influx most compatible with high performance AT scenarios. A new divertor will serve as an important test of the improved understanding gained through the enhancements, experiments, and model validation activities carried out over the next five years. Improved boundary models will guide future design for the lower divertor, which is expected to combine the salient features from the prior systematic divertor optimization studies. These include:

- Divertor target and baffle structure, gas injection and particle pumping for improved control of recycling neutral fueling and any seeded impurities required;
- A configuration designed to work with high performance core plasma scenarios;
- Compatibility with advanced divertor magnetic configurations examined during the exploratory phase of divertor concept optimization. Additional divertor poloidal field coils could be part of the design if warranted, though likely increasing costs significantly;
- More reactor relevant PFC materials and mitigation techniques to test compatiblility with high performance core plasmas. High temperature divertor components may be included if evidence from initial studies suggests a large effect on divertor operation and core plasma performance.

The realization of future upgrades is expected to provide a compelling test of concepts to achieve highly dissipative divertor operation at lower core plasma and impurity density for high performance core plasma operation.

Acknowledgments

This work was supported in part by the US Department of Energy under DE-AC02-09CH11466, DE-AC04-94AL85000, DE-AC05-00OR22725, DE-AC52-07NA273441, DE-FC02-04ER54698, and DE-FG02-07ER54917.

References

[1] Garofalo A.M. *et al* 2014 *Fusion Eng. Des.* **89** 876–81
[2] Chan V.S., Costley A.E., Wan B.N., Garofalo1 A.M. and Leuer J.A. 2015 *Nucl. Fusion* **55** 023017
[3] Buttery R.J. and the DIII-D Team 2015 *Nucl. Fusion* **55** 104017
[4] McLean A.G. *et al* 2015 Drift-driven divertor asymmetries in the transition from attached to fully detached conditions *57th Annual APS Meeting Division of Plasma Physics (Savannah, Georgia, 16–20 November 2015)* (http://meetings.aps.org/Meeting/DPP15/Session/VI2.1)
[5] Rognlien T.D. *et al* 2015 Modeling detached divertor plasma characteristics in the DIII-D Tokamak *57th Annual APS Meeting Division of Plasma Physics (Savannah, Georgia, 16–20 November 2015)* (http://meetings.aps.org/Meeting/DPP15/Session/CO6.13)
[6] Briesemeister A.R. *et al* 2015 Reduction in resonant magnetic field induced heat flux splitting caused by detachment of the divertor *57th Annual APS Meeting Division of Plasma Physics (Savannah, Georgia, 16–20 November 2015)* (http://meetings.aps.org/Meeting/DPP15/Session/CO6.14)
[7] Jakuboski M.W. *et al* 2009 *Nucl. Fusion* **49** 095013
[8] Groth M. *et al* 2011 *J. Nucl. Mater.* **415** S530
[9] Canik J.M. *et al* 2015 *J. Nucl. Mater.* **463** 569
[10] Tobita K. *et al* 2009 *Nucl. Fusion* **49** 075029
[11] Ryutov D.D. 2007 *Phys. Plasmas* **14** 064502
[12] Ryutov D.D., Cohen R.H., Farmer W.A., Rognlien T.D. and Umansky M.V. 2014 *Phys. Scr.* **89** 088002
[13] Kotschenreuther M., Valanju P., Wiley J., Rognlein T., Mahajan S. and Pekker M. 2004 Scrape Off Layer Physics for Burning Plasmas and Innovative Divertor Solutions *Proc. of the 20th Int. Conf. on Fusion Energy (Vilamoura, Portugal)* (Vienna: International Atomic Energy Agency) IC/P6–43 (www-naweb.iaea.org/napc/physics/fec/fec2004/datasets/IC_P6-43.html)
[14] Valanju P.M., Kotschenreuther M., Mahajan S.M. and Canik J. 2009 *Phys. Plasmas* **16** 056110
[15] LaBombard B. *et al* 2015 *Nucl. Fusion* **55** 053020
[16] Soukhanovskii V.A. *et al* 2014 Developing physics basis for the radiative snowflake divertor at DIII-D *Proc. 25th IAEA Int. Conf. on Fusion Energy (St. Petersburg, Russian Federation 13–18 October 2014)* EX/7-4 (Vienna: International Atomic Energy Agency) (www-naweb.iaea.org/napc/physics/FEC/FEC2014/fec_sourcebook_online.pdf)
[17] Kolemen E. *et al* 2015 Heat flux management via advanced magnetic divertor configurations and divertor detachment *J. Nucl. Mater.* **463** 1186
[18] Covele B. *et al* 2015 X-divertors for deeper detachment without degrading the DIII-D H-mode *57th Annual APS Meeting Division of Plasma Physics (Savannah, Georgia, 16–20 November 2015)* (http://meetings.aps.org/Meeting/DPP15/Session/TP12.73)
[19] Loarte A. 2001 Effects of divertor geometry on tokamak plasmas *Plasma Phys. Control. Fusion* **43** R183
[20] Kallenbach A. *et al* 1999 Scrape-off layer radiation and heat load to the ASDEX upgrade LYRA divertor *Nucl. Fusion* **39** 901
[21] Moser A.L. *et al* 2016 Effect of divertor closure on pedestal fueling and divertor detachmentonset in DIII-D *22nd Int. Conf. on Plasma Surface Interaction (Rome, May 2016)* (*J. Nucl. Mater. Energy* submitted) (http://psi2016.enea.it)
[22] Stangeby P.C. *et al* 2015 Two-point Analysis of SOLPS Modeling for a Slot Divertor *57th Annual APS Meeting Division of Plasma Physics (Savannah, Georgia, 16–20 November 2015)* (http://meetings.aps.org/Meeting/DPP15/Session/PM11.3)
[23] Kawashima H., Shimizu K., Takizuka T., Tobita K., Nishio S., Sakurai S. and Takenaga H. 2009 Simulation study for divertor design to handle huge exhaust power in the SlimCS DEMO reactor *Nucl. Fusion* **49** 065007
[24] Kukushkin A.S., Pacher H.D., Kotov V., Pacher G.W. and Reiter D. 2011 Finalizing the ITER divertor design: the key role of SOLPS modeling *Fusion Eng. Design* **86** 2865
[25] Sang C.F. *et al* 2015 SOLPS modeling of slot divertor configuration on DIII-D *57th Annual APS Meeting Division of Plasma Physics (Savannah, Georgia, 16–20 November 2015)* (http://meetings.aps.org/Meeting/DPP15/Session/TP12.77)
[26] Ding R. *et al* 2016 *Nucl. Fusion* **56** 016021
[27] Dux R. *et al* 2009 Plasma-wall interaction and plasma behaviour in the non-boronised all tungsten ASDEX upgrade *J. Nucl. Mater.* **390–1** 858
[28] van Rooij G.J. *et al* 2013 Tungsten divertor erosion in all metal devices: lessons from the ITER like wall of JET *J. Nucl. Mater.* **438** S42
[29] Abrams T. *et al* 2016 Impact of ELMs on the tungsten source distribution near the DIII-D outer strike point *22nd Int. Conf. on Plasma Surface Interaction (Rome, May 2016)* (*J Nucl. Mater. Energy* submitted) (http://psi2016.enea.it)